Original Article

Institution of MECHANICAL ENGINEERS
Journal of AEROSPACE ENGINEERING

Proc IMechE Part G:
J Aerospace Engineering
0(0) 1–11

DOI: 10.1177/0954410015603415
uk.sagepub.com/jaero
SAGE

A new approach in UAV path planning using Bezier–Dubins continuous curvature path

A Askari[1], M Mortazavi[1], HA Talebi[2] and A Motamedi[3]

Abstract

This paper presents continuous curvature paths for unmanned vehicles such as robots and unmanned aerial vehicles. The importance of these paths is that both upper-bounded curvature and upper-bounded curvature derivatives are included in the path. The approach is based on replacement of the Dubins line with the quintic PH Bezier curves by computing a shape parameter by considering the kinematic constraints of the path. Since these paths are Dubins-based paths, their lengths are close to the minimum length. The effectiveness and sub-optimality of the proposed paths are demonstrated through fully nonlinear simulation.

Keywords

Path planning, unmanned aerial vehicle, continuous curvature path, Dubins path, Bezier curve

Date received: 30 January 2015; accepted: 3 August 2015

Introduction

The route planning schemes such as those based on optimization methods and randomize search does not consider the kinematic constraints of the path. Therefore, the path should be smoothed by the curves, namely: Dubins path, kappa-trajectory, Bezier and PH Bezier curves, and Euler spirals. However, some of these methods such as Dubins[1] and kappa trajectory[2] suffer from discontinuity of the curvature.[3] On the other hand, there is no closed-form expression for the Bezier and spiral curves. In the Bezier curves, the curvature cannot be controlled and the control points must be placed in the appropriate position with trial and error. In the spiral curves, the position of the curves leads to Fresnel integrals. These integrals should be solved using a numerical method.[4]

Dubins path is the C^1 shortest path (a C^1 path is a path with slope continuity) joining two given directed points. The drawback of this path is the discontinuity of the curvature in the switching points.

The most complete work on the Dubins path is classified by Shkel and Lumelsky.[5] To find the shortest path, a decision table has been provided for different sets of initial and final configurations. Path planning of a miniature air vehicle (MAV) using Dubins has been presented by Hota and Ghose.[6] Then, the path has been modified in the presence of wind. Hota and Ghose also determined an optimal Dubins-based path for a 3D space.[7] An extended version of 2D Dubins for a 3D path generation of a group of UAVs has been proposed by Shanmugavel et al.[8,9] Babaei and Mortazavi have introduced two nonlinear equations to find the switching point of Dubins in 2D[10] and 3D,[11] respectively.

Dubins problem

Finding the shortest path between the initial and final configurations of a vehicle (such as robots) with the following kinematic equations

$$\begin{cases} \dot{x}(t) = V\cos\psi(t) \\ \dot{y}(t) = V\sin\psi(t) \\ \dot{\psi}(t) = \kappa(t) \quad , \ |\kappa(t)| < \kappa_{\max} \end{cases} \tag{1}$$

where V is the velocity, ψ is the heading angle, and κ is the curvature and also the control input.

[1]Aerospace Engineering Department, Amirkabir University of Technology, Tehran, Iran
[2]Electrical Engineering Department, Amirkabir University of Technology, Tehran, Iran
[3]Aerospace Engineering Department, K.N.Toosi University of Technology, Tehran, Iran

Corresponding author:
M Mortazavi, Aerospace Engineering Department, Amirkabir University of Technology, Hafez Ave. PO Box 15875-4413, Tehran, Iran.
Email: mortazavi@aut.ac.ir

If the speed is constant, the shortest path would be the shortest time using the following objective function

$$J = \int_0^T \mathrm{d}t \tag{2}$$

However, it should be noted that if a vehicle such as UAV is not able to stop at switching points, the dynamic has to be modified. An extended version of Dubins where a rear gear is added to the robot, has been solved by Reeds and Shepp.[12] To maintain continuity of the curvature, Scheuer et al. have done extensive research in this area based on the combination of clothoid curves with the Dubins path.[13–18] The results of this research introduce a seven pieces path including clothoid–circle–clothoid–line–clothoid–circle–clothoid for both forward and forward-backward motion. This sub-optimal path is a continuous curvature path with upper-bounded curvature derivatives. It has been shown that the deviation of the continuous curvature planned path from the followed path is less than that of the planned Dubins path from the followed path. Another subject which should be noted is that the Dubins solution (and also Reeds and Shepp) has some shortcomings, some of which can be addressed by appropriate assumptions. For example, in order to have an analytical solution, the speed of the vehicle is assumed to be constant. However, some assumptions such as discontinuity in the curvature profile are only correct for limited types of vehicles such as unconstrained or maneuverable robots.[17] It should be noted that following the continuous curvature paths is faster than following the Dubins path.[17] The reason is due to the time spent for stopping in the switching points and in this sense, for many vehicles, it is better to follow a class of C^2 paths (a C^2 path is a path whit both slope and curvature continuity). At the completion of the shortest path problem, Boissonnat have completed the dynamics of the vehicle as below[19]

$$\begin{cases} \dot{x}(t) = V\cos\psi(t) \\ \dot{y}(t) = V\sin\psi(t) \\ \dot{\psi}(t) = \kappa(t) \\ \dot{\kappa}(t) = \upsilon(t) \quad , \ |\upsilon(t)| < \upsilon_{\max} \end{cases} \tag{3}$$

where $\dot{\kappa}$ is the curvature derivative and it is also the control input.

Indeed, this is the generalized Dubins problem by considering an upper-bounded curvature derivative (but without the maximum curvature constraint). Using Pontryagin's Maximum Principle, by Boissonnat[19] and then Kostov[20] and Degtiariova-Kostova,[21] it has been shown that the shortest path is made up of the line segments and clothoid arcs of maximum curvature derivatives with an infinite number of switching points.

Bezier and Pythagorean hodograph Bezier curves

In recent years, an extensive research has been carried out in the Bezier and Pythagorean hodograph (PH) Bezier curves. The significance of this research is the possibility of using them in the path generation problem. The PH Bezier curve was first introduced by Farouki et al.[22] By definition, the Bezier curve $[z(t) = (x(t), y(t))]$ is said to be a PH curve if it satisfies a Pythagorean condition. PH curves with the ability of curvature control for some different sets of initial and final configurations using a C/S-shaped cubic Bezier curve have been presented by Walton and Meek.[23,24] An obstacle avoidance path smoothing technique by bounding the obstacle with a convex polygon and passing a C-shaped cubic Bezier curve on the vertices of the convex hull is presented by Li et al.[25] Then, Habib and Sakai have extended the research of Walton and Meek on planar transition between two circles by introducing a shape parameter m in the S/C-shaped cubic and PH quintic Bezier curves.[26,27] The advantage of this research is introducing a parameter m to re-shape the curves. Such that as m increases, the transition curve becomes tighter and as $m \to \infty$, the curve becomes a line and a Dubins path, of course, would be achieved. A 3D path generation of multiple UAVs using PH Bezier curves by considering the maximum curvature and torsion bounds has been done by Shanmugavel et al.[28] Then this approach is used for path generation of a MAV in an urban environment.[29]

The objective of this paper is introducing a class of new Dubins-based continuous curvature paths by a combination of the Dubins path and Bezier curves. The characteristics of the new paths are: (1) continuity in the curvature in the entire path, (2) upper-bounded curvature, (3) upper-bounded curvature derivative for vehicles, and (4) sub-optimality of the paths. The purpose of this study is combining the optimal Dubins path with the continuous PH Bezier curve to find a suboptimal continuous curvature path. PH curves with the ability of curvature control between two circles by introducing a shape parameter, m have been presented in Habib and Sakai.[27] Our innovation is introducing a criterion to select the optimum value of the shape parameter, m. It has been shown how the shape parameter, m is set in such a way that upper-bounded curvature derivative for a vehicle in order to guarantee a sub-optimal path, can be achieved. The new sub-optimal path has the properties of Dubins (path optimality) and the PH Bezier curves (curvature continuity). The contribution of this paper is the establishment of a logical connection between the dynamic capabilities of the vehicle and the kinematic constraints of the path. In this paper, the shortest quintic PH Bezier curve has been achieved. This work has been carried by taking into account the highest rate of the curvature of the PH Bezier curve that the vehicle can withstand.

This paper is organized as follows: The motivation behind this research is briefly given in the ''Problem statement'' section. In the ''Description of the method'', the proposed method of the continuous curvature path is presented in detail. In the ''Simulation'' section, simulation results are provided to illustrate the performance of the proposed approach. Some conclusions are given in the last section.

Problem statement

In this section, the general idea of producing a continuous curvature path using PH quintic Bezier curves has been introduced.

General idea

The joining of two circles using quintic PH Bezier curves has been performed by Habib and Sakai.[26,27] In these articles, a shape parameter, m has been introduced to re-shape the curve. Our approach is computing the shape parameter, m by considering the kinematic constraints of the path. Furthermore, knowing that the shortest path is the Dubins path, and by replacing the line in Dubins' with the Bezier curves, it is possible to generate a group of sub-optimal continuous curvature paths with an upper-bounded curvature derivative.

Bezier and Pythagorean Bezier curves

A quintic Bezier curve is given below[22]

$$\boldsymbol{z}(\boldsymbol{t}) = (x(t), y(t)) = \sum_{i=0}^{5} \binom{5}{i} \boldsymbol{P_i}(1-t)^{5-t} t^i, \quad 1 \geqslant t \geqslant 0 \tag{4}$$

where

$$\binom{n}{k} = \frac{n!}{k!(n-k)!} \tag{5}$$

A Bezier curve is a PH Bezier curve, if $[(\mathrm{d}x/\mathrm{d}t)^2+(\mathrm{d}y/\mathrm{d}t)^2]$ can be displayed as a square of a polynomial. To ensure this, they are defined as[22]

$$\begin{cases} \dot{x}^t(t) = \mathrm{d}x/\mathrm{d}t = u^2(t) - v^2(t) \\ \dot{y}^t(t) = \mathrm{d}y/\mathrm{d}t = 2u(t)v(t) \end{cases} \tag{6}$$

where

$$\begin{cases} u(t) = u_0(1-t)^2 + 2u_1 t(1-t) + u_2 t^2 \\ v(t) = v_0(1-t)^2 + 2v_1 t(1-t) + v_2 t^2 \end{cases} \tag{7}$$

The control points $\boldsymbol{P_i}$ are defined as[22]

$$\begin{cases} \boldsymbol{P_0} = (0,0) \\ \boldsymbol{P_1} = \boldsymbol{P_0} + \frac{1}{5}\left(u_0^2 - v_0^2, 2u_0 v_0\right) \\ \boldsymbol{P_2} = \boldsymbol{P_1} + \frac{1}{5}(u_0 u_1 - v_0 v_1, u_0 v_1 + u_1 v_0) \\ \boldsymbol{P_3} = \boldsymbol{P_2} + \frac{1}{15}\left(2u_1^2 - 2v_1^2 + u_0 u_2 - v_0 v_2,\right. \\ \qquad \left. 4u_1 v_1 + u_0 v_2 + u_2 v_0\right) \\ \boldsymbol{P_4} = \boldsymbol{P_3} + \frac{1}{5}(u_1 u_2 - v_1 v_2, u_1 v_2 + u_2 v_1) \\ \boldsymbol{P_5} = \boldsymbol{P_4} + \frac{1}{5}\left(u_2^2 - v_2^2, 2u_2 v_2\right) \end{cases} \tag{8}$$

One of the important advantages of the PH Bezier curve as compared to a Bezier curve is that the total length of the PH curve can be expressed in a closed form. The total length of a curve is

$$S_f = \int_0^1 \sqrt{(\mathrm{d}x/\mathrm{d}t)^2+(\mathrm{d}y/\mathrm{d}t)^2}\,\mathrm{d}t \tag{9}$$

By substitution of $\dot{x}^t$ and $\dot{y}^t$ in equation (9), rearranging and integrating, the total length of a quintic PH curve can be obtained as

$$\begin{aligned} S_f = {} & \frac{u_0^2}{5} + \frac{u_0 u_1}{5} + \frac{u_0 u_2}{15} + 2\frac{u_1^2}{15} + \frac{u_1 u_2}{5} + \frac{u_2^2}{5} + \frac{v_0^2}{5} \\ & + \frac{v_0 v_1}{5} + \frac{v_0 v_2}{15} + 2\frac{v_1^2}{15} + \frac{v_1 v_2}{5} + \frac{v_2^2}{5} \end{aligned} \tag{10}$$

The closed form expression of the length is useful for the proposed algorithm in this article.

Description of the method

In this section, two algorithms of the continuous curvature paths will be presented, which are C/S-shaped quintic PH Bezier curves.

Definitions and abbreviations

The subscripts (superscripts) ''i'', ''f'', ''r'', ''l'' stand for ''initial'', ''final'', ''right'', and ''left'', respectively. $\boldsymbol{C_i}$ and $\boldsymbol{C_f}$ are the initial and final center of the circles, and $(\boldsymbol{P_i}, \alpha)$ and $(\boldsymbol{P_f}, \beta)$ are the initial and final configurations. r_i and r_f are the initial and final minimum turning radius. Without the loss of generality, in this paper, it is assumed that $r_i = r_f$. $r = \|\boldsymbol{C_i} - \boldsymbol{C_f}\|$ is the distance between $\boldsymbol{C_i}$ and $\boldsymbol{C_f}$, S_f is the total length of the curve, and $\overline{\boldsymbol{C_i}\boldsymbol{C_f}}$ is the line connecting the initial and final center of the circles. In this article, in order to avoid ambiguity, define ''t'' as time and ''t''—in the Italic form—as the curve parameter in the Bezier equations. Define $\dot{\kappa} = \frac{\partial \kappa}{\partial t}$ (the time derivative of the curvature), $\dot{\kappa}^t = \frac{\partial \kappa}{\partial t}$ (''t'' – the curve parameter in the Bezier equations), and $\dot{\kappa}^s = \frac{\partial \kappa}{\partial s}$ (''s'' - the length of the curve). $\dot{\kappa}^s$ can be derived from the vehicle

performance. The relationship between the curvature and performance of the vehicle is as follows

$$\kappa = \frac{\dot{\psi}}{V} \tag{11}$$

where κ is the curvature of the path, $\dot{\psi}$ is the derivative of the vehicle heading angle with respect to time, and V is the vehicle velocity (which is supposed to be constant). Taking derivatives from both sides of equation (11) yields in

$$\dot{\kappa} = \frac{\ddot{\psi}}{V} \tag{12}$$

On the other hand, using the chain rule

$$\dot{\kappa}^s = \frac{\partial \kappa}{\partial s} = \frac{\partial \kappa}{\partial t} \cdot \frac{\partial t}{\partial s} = \frac{\dot{\kappa}}{V} \tag{13}$$

By combination of equations (12) and (13), the relationship between the curvature derivative and the angular acceleration of the vehicle would be obtained as

$$\dot{\kappa}^s = \frac{\ddot{\psi}}{V^2} \tag{14}$$

Besides, the relation between t (the parameter in the Bezier) and s (the length of the curve) is as follows

$$t = \frac{s}{S_f} \rightarrow dt = \frac{ds}{S_f} \tag{15}$$

Therefore

$$\dot{\kappa}^s = \frac{1}{S_f}\dot{\kappa}^t \tag{16}$$

The algorithm of the PH quintic S-shaped Bezier curve

1. Assumptions are summarized in Table 1.
2. $\boldsymbol{P_i} = (0,0)$ is chosen on the origin. Otherwise, translation is necessary such that $\boldsymbol{C_i} = (0, r_i)$.
3. In case $\kappa_i = -1/r_i$, $\kappa_f = +1/r_f$, the desired curve according to Figure 1, can be obtained by reflection of the curve relative to line $\overline{\boldsymbol{C_iC_f}}$.
4. The parameters u_0, u_1, u_2 and v_0, v_1, v_2 in equation (8) are as below[27]

$$\begin{cases} (u_0, u_1, u_2) = u_0\left(1, \frac{3m}{4}, 1\right), & m \geqslant 1, \quad u_0 > 0 \\ (v_0, v_1, v_2) = \left(0, \frac{u_0^3}{4r_i}, 0\right) \end{cases} \tag{17}$$

Table 1. Requirements of construction of quintic S-shaped PH Bezier curve.

1. $r_i = r_f$
2. $r = \|\boldsymbol{C_i} - \boldsymbol{C_f}\|$, $r > r_i + r_f$
3. $\boldsymbol{P_0} = (0,0)$
4. $\boldsymbol{C_i} = (0, r_i)$
5. $\boldsymbol{C_f} = \boldsymbol{P_5} - (0, r_f)$
6. $\overline{\boldsymbol{P_0P_1}}, \overline{\boldsymbol{P_4P_5}} \| (1,0)$: it means that $(\boldsymbol{P_1} - \boldsymbol{P_0})$ and $(\boldsymbol{P_5} - \boldsymbol{P_4})$ are parallel to x-axis
7. $\kappa_i = 1/r_i$, $\kappa_f = -1/r_f$

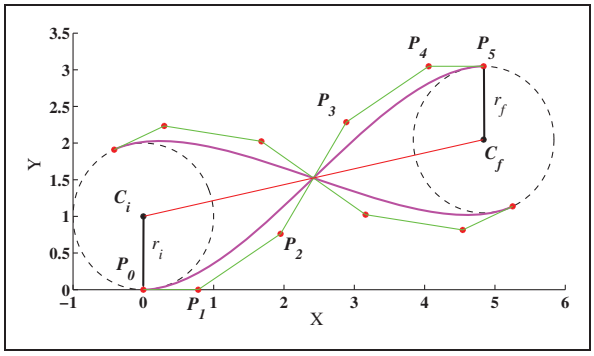

Figure 1. S-shaped curve and its reflection relative to the line$\overline{\boldsymbol{C_iC_f}}$.

u_0 is determined from equation $[f(u_0) = 0]$, which is as follows[27]

$$\begin{aligned} f(u_0) = {} & u_0^{12} + 2r_i^2\{9m^2 + 36m + 16\}u_0^8 \\ & + r_i^4\{81m^4 + 648m^3 + 2304m^2 - 1472\}u_0^4 \\ & - 14400r_i^4\{r^2 - 4r_i^2\} \end{aligned} \tag{18}$$

There is just one positive value of u_0^4 and therefore, this ensures a unique solution for u_0.

5. The quintic PH Bezier curve can be coincident with the Dubins path by rotation equal to $\theta_{rotation}$ around $\boldsymbol{C_i}$ and translation equal to $d_{translation}$ (Figure 2).
6. The parameter m to have the maximum curvature derivative for the quintic Bezier curve is determined using the following lemma.

Lemma 1. The maximum m for the S-shaped quintic Bezier curve at $t = 0$ is as follows

$$m_{\max}|_{t=0} = \frac{1}{6} r_i . S_f . \dot{\kappa}^s_{\max} + 1 \tag{19}$$

(Proof: see Appendix).

The result has been shown in Figure 3(a) to (c) with $m_{\max} = 1.74$.

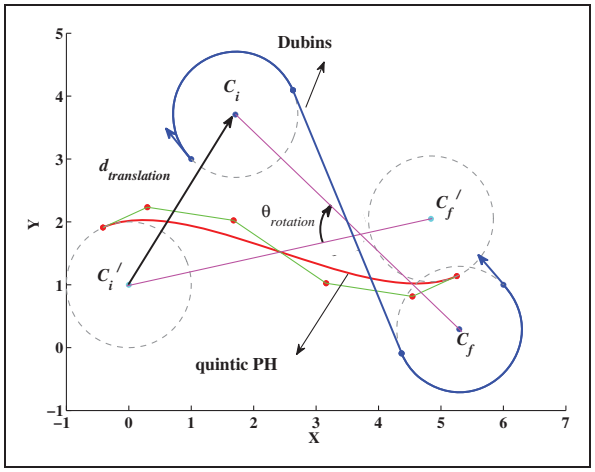

Figure 2. Rotation and translation to coincident the quintic PH Bezier curve on Dubins.

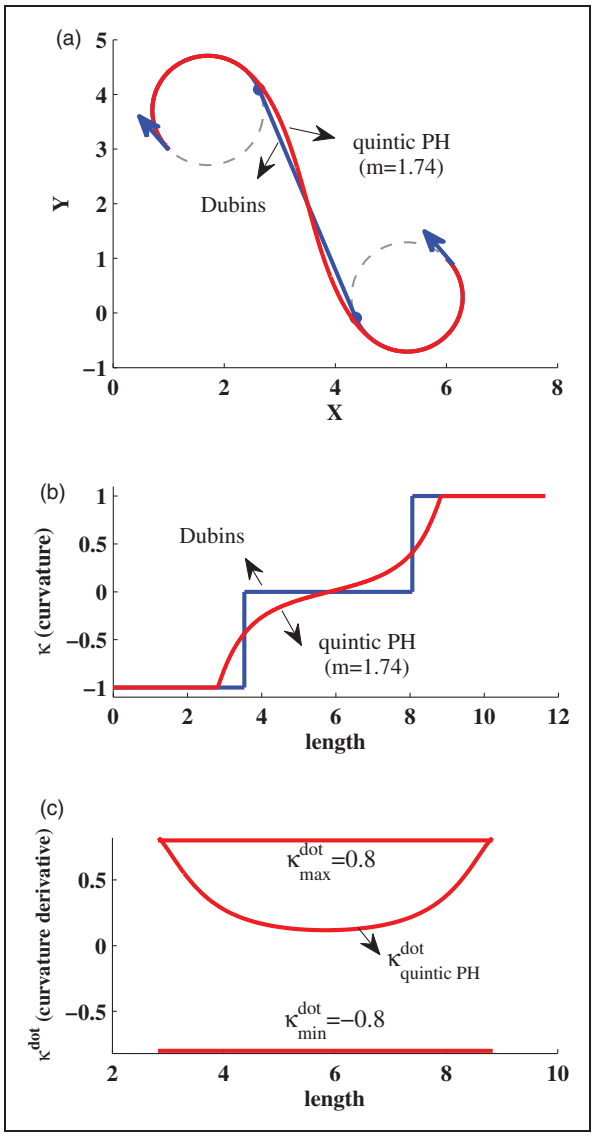

Figure 3. S-shaped Dubins and quintic PH Bezier curve ($m = 1.74$).: (a) Dubins and quintic PH Bezier curve ($m = 1.74$); (b) Curvature of Dubins and quintic PH curve ($m = 1.74$); (c) Curvature derivative of the quintic PH Bezier curve.

Table 2. Requirements of construction of quintic C-shaped PH Bezier curve.

1. $r_i = r_f$
2. $r = \|\boldsymbol{C_i} - \boldsymbol{C_f}\|$, $r > r_i - r_f$
3. $\boldsymbol{P}_0 = (0,0)$
4. $\boldsymbol{C_i} = (0, r_i)$
5. $\overline{\boldsymbol{P_0P_1}}, \overline{\boldsymbol{P_4P_5}} \| (1,0)$: it means that $(\boldsymbol{P}_1 - \boldsymbol{P}_0)$ and $(\boldsymbol{P}_5 - \boldsymbol{P}_4)$ are parallel to x-axis
6. $\kappa_i = 1/r_i$, $\kappa_f = 1/r_f$

The Algorithm of the PH quintic C-shaped Bezier curve

1. Assumptions are summarized in Table 2.
2. $\boldsymbol{P_i} = (0,0)$ is chosen on the origin. Otherwise, translation is necessary such that $\boldsymbol{C_i} = (0, r_i)$.
3. In case $\kappa_i = -1/r_i$, $\kappa_f = -1/r_f$, the desired curve can be obtained by reflection of the curve relative to line $\overline{\boldsymbol{C_iC_f}}$.
4. The parameters u_0, u_1, u_2 and v_0, v_1, v_2 (equation (8)) are as below[27]

$$\begin{cases} (u_0, u_1, u_2) = 2\sqrt{m.r_i.\tan\theta}(1, m, \cos 2\theta), \ m \geqslant 1 \\ (v_0, v_1, v_2) = 2\sqrt{m.r_i.\tan\theta}(0, m.\tan\theta, \sin 2\theta) \end{cases} \tag{20}$$

By considering $q = \tan^2\theta$:

$$\begin{cases} (u_0, u_1, u_2) = 2\sqrt{m.r_i.\sqrt{q}}\left(1, m, \frac{1-q}{1+q}\right), \ m \geqslant 1 \\ (v_0, v_1, v_2) = 2\sqrt{m.r_i.\sqrt{q}}\left(1, m\sqrt{q}, \frac{2\sqrt{q}}{1+q}\right) \end{cases} \tag{21}$$

q is determined from equation $g(q) = 0$, which is[27]

$$\begin{aligned} g(q) &= \sum_{i=0}^{5} d_i q^i \quad , \\ d_5 &= 64m^6 r_i^2 \\ d_4 &= 64m^4 r_i^2 \{4m^2 + 6m - 5\} \\ d_3 &= 16m^2 r_i^2 (24m^4 + 72m^3 + 24m^2 - 95) \\ d_2 &= -225r^2 + 32r_i^2(8m^6 + 36m^5 + 54m^4 \\ &\quad - 48m^3 - 125m^2 + 75) \\ d_1 &= -450r^2 + 16r_i^2(4m^6 + 24m^5 + 64m^4 + 24m^3 \\ &\quad - 131m^2 - 210 + 225) \\ d_0 &= -225r^2 \end{aligned} \tag{22}$$

There is just one positive value of $q = \tan^2\theta$ and, therefore, this ensures a unique solution for θ.

5. The center of the final circle is given by

$$\boldsymbol{C_f} = \boldsymbol{P}_5 + \begin{pmatrix} -r_f.\sin 4\theta \\ r_f.\cos 4\theta \end{pmatrix} \tag{23}$$

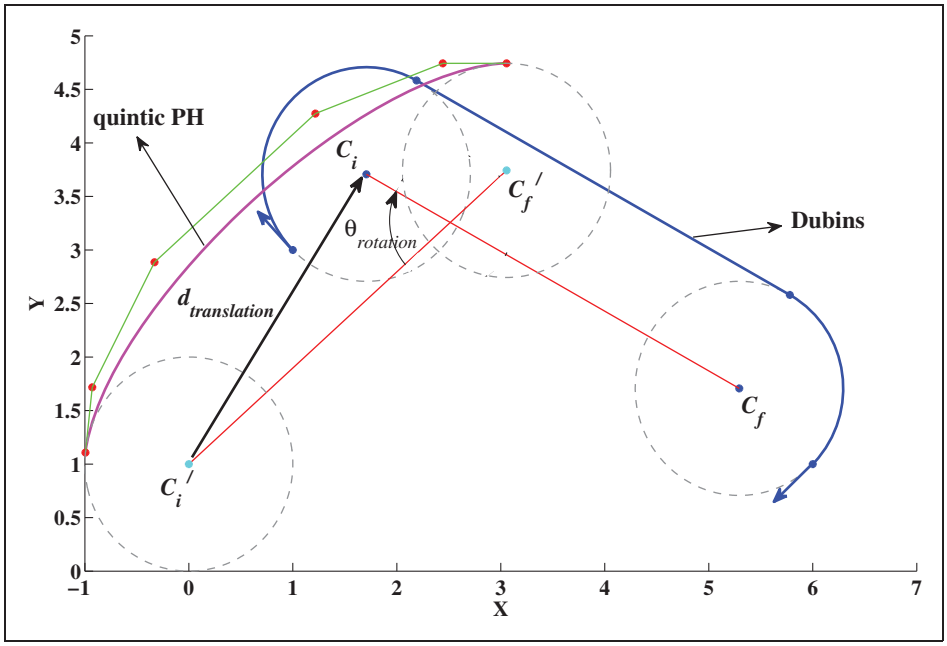

Figure 4. Rotation and translation to coincident the quintic PH Bezier curve on the Dubins.

6. The quintic PH Bezier curve can be coincident with the Dubins by rotation equal to $\theta_{rotation}$ around C_i' and translation equal to $d_{translation}$ (Figure 4).
7. The parameter m to have the maximum curvature derivative for the C-shaped quintic Bezier curve is determined using the following lemma.

Lemma 2. The maximum m for the C-shaped quintic Bezier curve at $t = 0$ is determined from the following equation

$$\left| m^2 - \frac{3}{6}m - \frac{1}{4(1+q)} \right| + \frac{r_i S_f . \dot{\kappa}^s_{\max}}{8} m = 0, \qquad m \geqslant 1 \tag{24}$$

(Proof: see Appendix).

The result has been shown in Figure 5(a) to (c) with $m_{\max} = 1.56$. Because a closed-form expression of S_f has been introduced in equation (10), there is no need for an iteration to determine the value of m. Besides, as shown in Figure 5(c), the maximum m for the quintic PH Bezier curve happens at $t = 0$.

Remark. For a PH Bezier curve, it is possible to relate the total length of the curve in a closed form expression and therefore, the parameter m has been determined in an explicit form.

It is fortunately mentioned that the parameter m is a function of the kinematic constraints of the vehicle, r_i and $\dot{\kappa}^s_{\max}$. Therefore, in case where $r = \|C_i - C_f\|$ is constant, the parameter m—for a vehicle—should be determined only once.

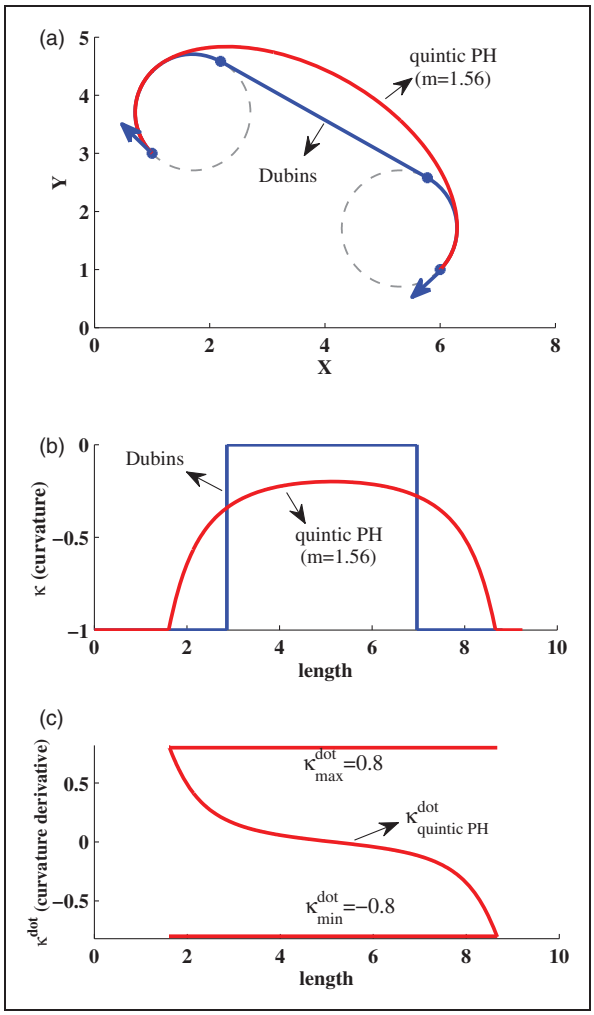

Figure 5. C-shaped Dubins and quintic PH Bezier curve ($m = 1.56$). (a) Dubins and quintic PH Bezier curve ($m = 1.56$); (b) Curvature of Dubins and quintic PH Bezier curve ($m = 1.56$); (c) curvature derivative of the quintic PH Bezier cure ($m = 1.56$).

A comparison between the length of the Dubins and Bezier paths has been shown in Tables 3 and 4. Since the proposed paths are Dubins-based continuous curvature paths, it can be said that these paths are sub-optimal. As can be seen in the following tables, increasing the length of the proposed paths compared to Dubins' is almost negligible.

Simulation results

The proposed continuous curvature paths are applied to UAV path planning in the presence of the obstacles. The UAV used for case studies is a turbojet powered UAV.[30] The Dijkstra search algorithm[31] has been used in a 2D search area $80 \times 30\,\text{km}^2$ to find the optimal path, while the altitude is assumed to be constant ($h = 1700\,\text{m}$). The optimal path, and smoothed Dubins and new paths have been illustrated in Figure 6.

The pure pursuit guidance law is applied for following the waypoints[32]

$$a_{pp} = \frac{N(V_I \times R) \times R}{V_I R} \rightarrow a_{lat} = a_{pp}(2) \tag{25}$$

Table 3. Comparison of S-shaped paths.

	Dubins (reference)	Quintic PH Bezier
Length	11.59	11.64
ΔL (%)	–	0.45

Table 4. Comparison of C-shaped paths.

	Dubins (reference)	Quintic PH Bezier
Length	8.81	9.25
ΔL (%)	–	4.9

Where N is the pure pursuit coefficient, R is the line of sight (LOS) vector and V_I is the UAV's velocity vector in the inertial system (Figure 7).

The UAV control system is a PID-based autopilot for the altitude, bank angle, and speed. The linear lateral-directional equation of the aircraft is expressed as[33]

$$a_y = \dot{v} + U_1 r = g\varphi\cos\theta_1 + Y_\beta\beta + Y_p p + Y_r r + Y_{\delta_A}\delta_A + Y_{\delta_R}\delta_R \tag{26}$$

$$\dot{p} - \frac{I_{xz}}{I_{xx}}\dot{r} = L_\beta\beta + L_p p + L_r r + L_{\delta_A}\delta_A + L_{\delta_R}\delta_R \tag{27}$$

$$\dot{r} - \frac{I_{xz}}{I_{zz}}\dot{p} = N_\beta\beta + N_p p + N_r r + N_{\delta_A}\delta_A + N_{\delta_R}\delta_R \tag{28}$$

where v, φ, p, r, and β are lateral-directional state variables: lateral speed, bank angle, roll rate, yaw rate, and side slip angle, respectively. δ_A and δ_R are control inputs: aileron and rudder deflections, respectively. a_y is the side acceleration, and U_1 and θ_1 are steady-state velocity and pitch angle of the UAV, respectively. For the UAV in this research, $Y_{\delta_A} = 0$.[30] Furthermore, the rudder is assumed to be inactive, i.e. $\delta_R = 0$. Therefore, from equation (26) the bank angle can be expressed as follows

$$\varphi = \frac{1}{g\cos\theta_1}[a_{lat_{Guidance}} - Y_\beta\beta - Y_p p - Y_r r] \tag{29}$$

This is a model inversion and therefore, the stability of the internal dynamic equations (27) and (28) should be verified.[34] However, the stability of the internal dynamic has been guaranteed in the design of the bank angle mode autopilot.

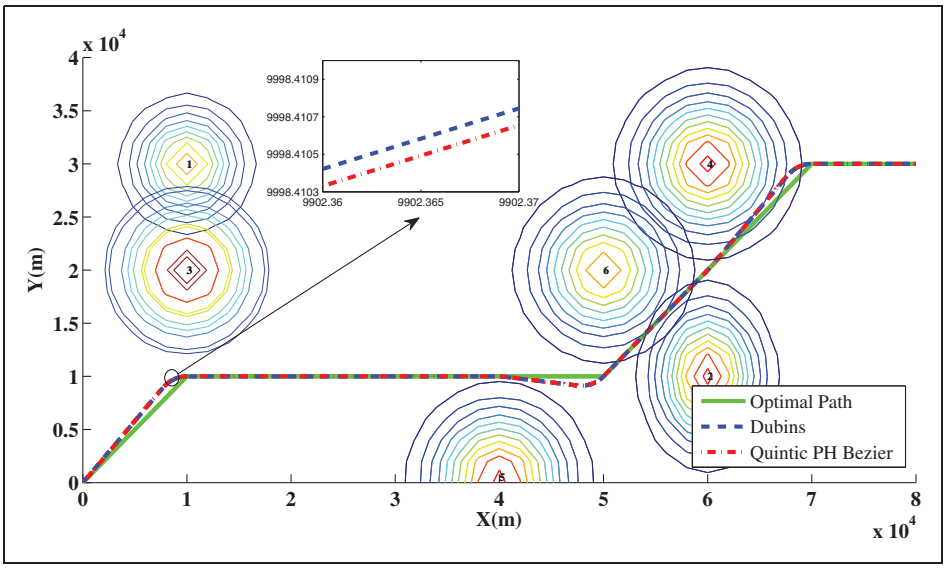

Figure 6. The optimal and smoothed PH Bezier path.

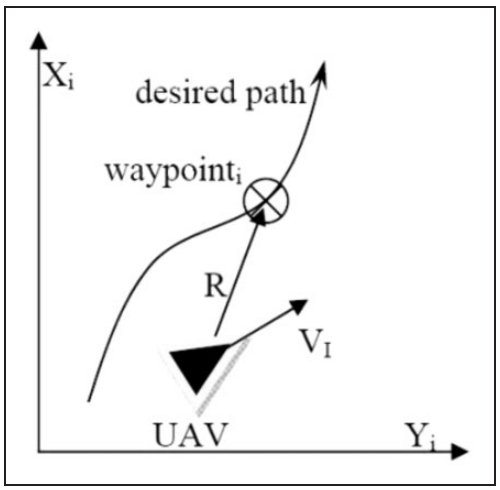

Figure 7. The position of UAV and the desired path.

Figure 8(a) and (b) shows the simulation of the path planning for the Dubins and Bezier curves. Orientation of the UAV at initial point (0,0,1700) is deliberately considered to be different from the orientation of the designed path. According to Figure 8(a) and (b), it is shown that the optimal and followed paths have a good compliance and therefore, the guidance and control system executed a good chasing. Comparisons between the length of the designed and followed paths are summarized in Table 5. Although the new designed paths are sub-optimal, it is shown that following the new continuous curvature path are more accurate and they have less deviation than that the discontinuous optimal Dubins path (Figure 8(a) and (b)). Figure 6 shows that the differences between the new designed path and the Dubins' are negligible, while Figure 8(a) and (b) shows tracking the

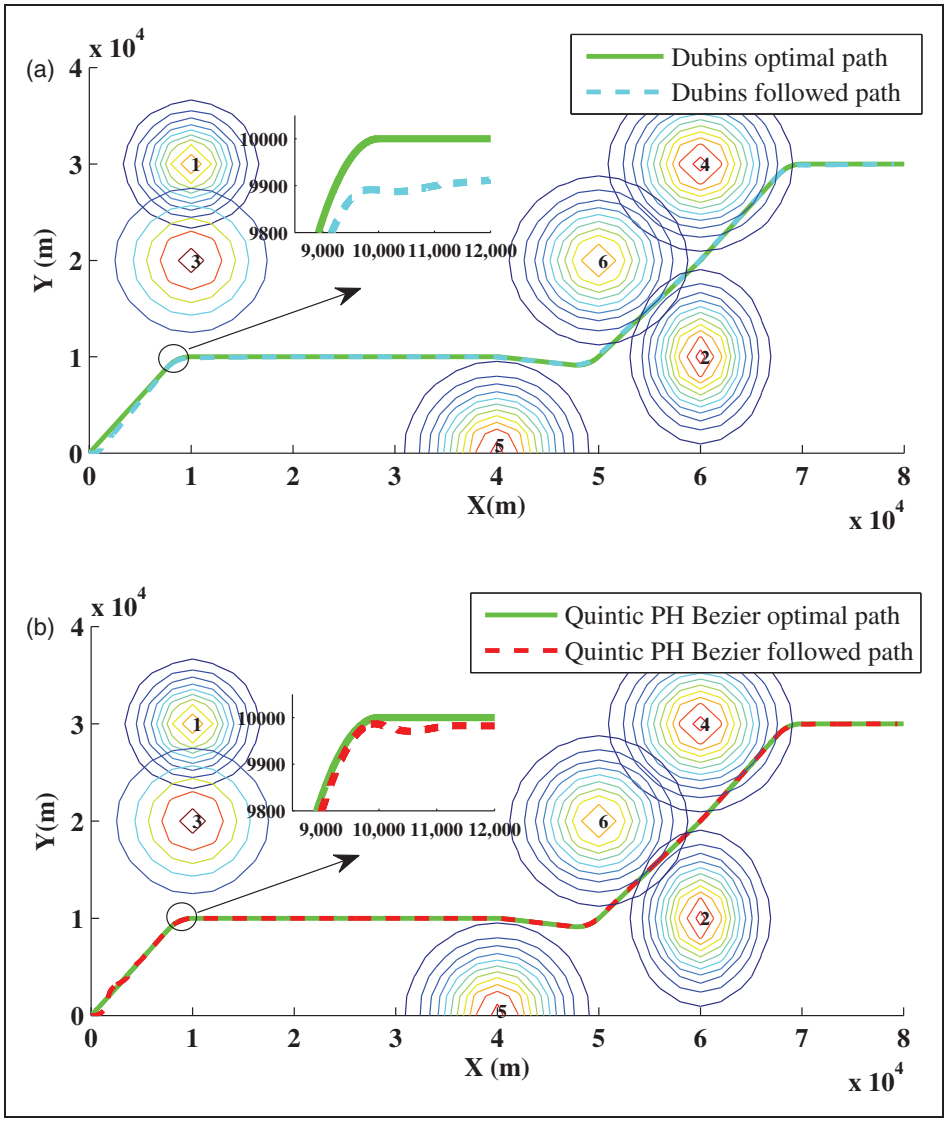

Figure 8. The optimal and followed Dubins and quintic PH Bezier paths. (a) Dubins optimal and followed path; (b) Quintic PH Bezier optimal and followed Path.

Table 5. Comparison of the designed and followed paths.

Length (m)	Dubins	Quintic PH Bezier
Length of design path	93,246	94,421
Length of followed path	99,486	98,282
Deviation(%)	6.7	4.1

continuous curvature path results in less deviation from the designed path. Precisely speaking, according to Table 5, the length difference of the designed continuous curvature path from the designed Dubins' is about 1.2%. Whereas following the quintic PH Bezier paths are about 2.6% more accurate than following the Dubins'. Therefore, it should be noted that in the quintic PH Bezier curve, in addition to control the curvature derivative, it has more fairness than the Dubins'. Thus tracking the quintic PH Bezier path is expected to be more accurate than tracking the Dubins path (Figure 8(a) and (b)). Table 5 shows that tracking the quintic Bezier is more accurate and it has less deviation. Actually, if the Dubins followed path is considered as a reference path, it should be noted that the quintic PH Bezier Dubins-based path causes the length of the reference path to be shorter about 1.2%.

It should be mentioned that the shape parameter, m need to be calculated only once for a vehicle. Since then, the speed of producing the new path is equal to Dubins' and therefore, this method can be used both offline and online.

Conclusions

In this paper, continuous curvature curves using quintic PH Bezier curve has been introduced. The approach is based on combination of the Dubins path and the Bezier curves by replacing the Dubins line with the Bezier curves. However, for a vehicle, a continuous curvature curve is a necessary condition and the sufficient condition is an adaptation of the curvature derivative of the path with the vehicle angular acceleration. It has been shown that unlike the Dubins path, it is possible to control the curvature derivative of the proposed new paths using the shaped parameter.

With this description, using the fully nonlinear simulation, it has been shown that the shortest Dubins path is not necessarily the shortest implemented path. Therefore, there is no adequate executive guarantee in order to have an appropriate compliance between the planned and the followed paths. The issue that should be considered is that the deviation of a vehicle from the designed path in a real maneuver indicates the degree of importance of the produced route. It means the precision in the maneuver implementation shows the credit rating of a designed path. The results showed that the continuous curvature paths (quintic Bezier curves) have higher credit rating than the discontinuous curvature Dubins path.

Conflict of interest

The authors declared no potential conflicts of interest with respect to the research, authorship, and/or publication of this article.

Funding

The authors received no financial support for the research, authorship, and/or publication of this article.

References

1. Dubins LE. On curves of minimal length with a constraint on average curvature, and with prescribed initial and terminal positions and tangents. *Am J Math* 1957; 79: 497–516.
2. Anderson EP, Beard RW and McLain TW. Real-time dynamic trajectory smoothing for unmanned air vehicles. *IEEE Trans Control Syst Technol* 2005; 13: 471–477.
3. Shanmugavel M. *Path planning of multiple autonomous vehicles*. PhD Thesis, University of Cranfield, UK, 2007.
4. Tsourdos A, White B and Shanmugavel M. *Cooperative path planning of unmanned aerial vehicles*. New York: John Wiley & Sons, 2010.
5. Shkel AM and Lumelsky V. Classification of the Dubins set. *Robot Autonom Syst* 2001; 34: 179–202.
6. Hota S and Ghose D. A modified Dubins method for optimal path planning of a miniature air vehicle converging to a straight line path. In: *2009 ACC'09 American control conference*, 2009, pp.2397–2402. New York: IEEE.
7. Hota S and Ghose D. Optimal geometrical path in 3D with curvature constraint. In: *The 2010 IEEE/RSJ International conference on intelligent robots and systems (IROS)*, 2010, pp.113–118. New York: IEEE.
8. Shanmugavel M, Tsourdos A, White BA, et al. 3D Dubins sets based coordinated path planning for swarm of UAVs. In: *AIAA Guidance, navigation, and control conference and exhibit*, August 2006, Keystone, Colorado.
9. Shanmugavel M, Tsourdos A, White B, et al. Co-operative path planning of multiple UAVs using Dubins paths with clothoid arcs. *Control Eng Pract* 2010; 18: 1084–1092.
10. Babaei AR and Mortazavi M. Fast trajectory planning based on in-flight waypoints for unmanned aerial vehicles. *Aircraft Eng Aerosp Technol* 2010; 82: 107–115.
11. Babaei AR and Mortazavi M. Three-dimensional curvature-constrained trajectory planning based on in-flight waypoints. *J Aircraft* 2010; 47: 1391–1398.
12. Reeds J and Shepp L. Optimal paths for a car that goes both forwards and backwards. *Pacific J Math* 1990; 145: 367–393.
13. Scheuer A and Fraichard T. Planning continuous-curvature paths for car-like robots. In: *Proceedings of the 1996 IEEE/RSJ international conference on intelligent robots and systems*, 1996, pp.1304–1311. New York: IEEE.

14. Scheuer A and Fraichard T. Collision-free and continuous-curvature path planning for car-like robots. In: *Proceedings of the 1997 IEEE international conference on robotics and automation*, 1997, pp.867–873. New York: IEEE.
15. Scheuer A and Fraichard T. Continuous-curvature path planning for car-like vehicles. In: *Proceedings of the 1997 IEEE/RSJ international conference on intelligent robots and systems*, 1997, pp.997–1003. New York: IEEE.
16. Scheuer A and Laugier C. Planning sub-optimal and continuous-curvature paths for car-like robots. In: *Proceedings of the 1998 IEEE/RSJ international conference on intelligent robots and systems*, 1998, pp.25–31. New York: IEEE.
17. Scheuer A and Xie M. Continuous-curvature trajectory planning for manoeuvrable non-holonomic robots. In: *Proceedings of the 1999 IEEE/RSJ international conference on intelligent robots and systems*, 1999, pp.1675–1680. New York: IEEE.
18. Fraichard T and Scheuer A. From Reeds and Shepp's to continuous-curvature paths. *IEEE Trans Robot* 2004; 20: 1025–1035.
19. Boissonnat J-D, Cerezo A and Leblond J. A note on shortest paths in the plane subject to a constraint on the derivative of the curvature. INRIA, Institut National de Recherche en Informatique et Automatique, 1994.
20. Kostov V and Degtiariova-Kostova E. Some properties of clothoids. Research Report 2752, Institut National de Recherche en Informatique et Automatique, 1995.
21. Kostov V and Degtiariova-Kostova E. Irregularity of optimal trajectories in a control problem for a car-like robot. Research Report 3411, Institut National de Recherche en Informatique et Automatique, 1998.
22. Farouki RT and Sakkalis T. Pythagorean hodographs. *IBM J Res Develop* 1990; 34: 736–752.
23. Walton DJ and Meek DS. Planar G2 curve design with spiral segments. *Comput-Aided Des* 1998; 30: 529–538.
24. Walton DJ and Meek DS. Planar G2 transition between two circles with a fair cubic Bézier curve. *Comput-Aided Des* 1999; 31: 857–866.
25. Li Z, Meek DS and Walton DJ. A smooth, obstacle-avoiding curve. *Comput Graph* 2006; 30: 581–587.
26. Habib Z and Sakai M. G2 cubic transition between two circles with shape control. *J Comput Appl Math* 2009; 223: 133–144.
27. Habib Z and Sakai M. G2 Pythagorean hodograph quintic transition between two circles with shape control. *Comput-Aided Geometr Des* 2007; 24: 252–266.
28. Shanmugavel M, Tsourdos A and White BA. 3D path planning for multiple UAVs using Pythagorean hodograph curves. In: *AIAA Guidance, navigation and control conference and exhibit*, August 2007, Hilton Head, South Carolina.
29. Shanmugavel M, Tsourdos A and White BA. Collision avoidance and path planning of multiple UAVs using flyable paths in 3D. In: *15th International conference on methods and models in automation and robotics*, 2010, pp.218–222. New York: IEEE.
30. Askari A, Mortazavi M and Talebi H. UAV formation control via the virtual structure approach. *J Aerosp Eng* 2015; 28: 04014047.
31. Rippel E, Bar-Gill A and Shimkin N. Fast graph-search algorithms for general-aviation flight trajectory generation. *J Guid Control Dyn* 2005; 28: 801–811.
32. Enomoto K, Yamasaki T, Takano H, et al. Guidance and control system design for chase UAV. In: *Proceedings of GN & C conference, AIAA Paper*, August 2008, Honolulu, Hawaii.
33. Roskam J. *Airplane flight dynamics and automatic flight controls*. 1st ed. Kansas: Roskam Aviation and Engineering Corporation, 1995.
34. Khalil HK and Grizzle J. *Nonlinear systems*. Upper Saddle River: Prentice Hall, 2002.

Appendix

Proof of Lemma 1. The curvature and curvature derivative of a quintic PH Bezier curve are given by

$$\kappa = \frac{2(uv' - u'v)}{(u^2 + v^2)^2} \tag{30}$$

The derivative of the curvature with respect to parameter t yields in

$$\dot{\kappa}^t = \frac{2\{(uv'' - u''v)(u^2 + v^2) - 4(uv' - u'v)(uu' + vv')\}}{(u^2 + v^2)^3} \tag{31}$$

u and v and the first and second derivative of u and v for the S-shaped quintic PH Bezier curve are as below

$$\begin{cases} u(t) = u_0(1-t)^2 + 2u_1t(1-t) + u_2t^2 \\ u'(t) = -2u_0(1-t) - 4u_1t + 2u_2t + 2u_1 \\ u''(t) = 2u_0 - 4u_1 + 2u_2 \\ v(t) = v_0(1-t)^2 + 2v_1t(1-t) + v_2t^2 \\ v'(t) = -2v_0(1-t) - 4v_1t + 2v_2t + 2v_1 \\ v''(t) = 2v_0 - 4v_1 + 2v_2 \end{cases} \tag{32}$$

and for $t = 0$, it yields in

$$\begin{aligned} u(0) = u_0, u'(0) = -2u_0 + 2u_1 \\ u''(0) = 2u_0 - 4u_1 + 2u_2 \\ v(0) = v_0, v'(0) = -2v_0 + 2v_1 \\ v''(0) = 2v_0 - 4v_1 + 2v_2 \end{aligned} \tag{33}$$

The parameters u_0, u_1, u_2 and v_0, v_1, v_2 are as below

$$\begin{cases} (u_0, u_1, u_2) = u_0\left(1, \frac{3m}{4}, 1\right) \\ (v_0, v_1, v_2) = \left(0, \frac{u_0^3}{4r_i}, 0\right) \end{cases} \tag{34}$$

Substituting in $\dot{\kappa}^t$ and with a combination of equation (17) yields in

$$m_{max}|_{t=0} = \frac{1}{6} r_i . S_f . \dot{\kappa}^s_{max} + 1 \tag{35}$$

Proof of Lemma 2. The parameters u_0, u_1, u_2 and v_0, v_1, v_2 are as below

$$\begin{cases} (u_0, u_1, u_2) == 2\sqrt{m.r_i.\sqrt{q}}\left(1, m, \frac{1-q}{1+q}\right), \ m \geqslant 1 \\ (v_0, v_1, v_2) == 2\sqrt{m.r_i.\sqrt{q}}\left(1, m\sqrt{q}, \frac{2\sqrt{q}}{1+q}\right) \end{cases} \tag{36}$$

Substituting in $\dot{\kappa}^t$ and with a combination of equation (16) yields in

$$\left| m^2 - \frac{3}{6}m - \frac{1}{4(1+q)} \right| + \frac{r_i S_f . \dot{\kappa}^s_{max}}{8} m = 0 \tag{37}$$